Chemical and topographical modification of PHBV surface to promote osteoblast alignment and confinement

H. Kenar,[1] A. Kocabas,[2] A. Aydinli,[2] V. Hasirci[1]
[1]*METU, BIOMAT, Department of Biological Sciences, Biotechnology Research Unit, Ankara, Turkey*
[2]*Department of Physics, Bilkent University, Ankara 06800, Turkey*

Received 10 January 2007; revised 21 June 2007; accepted 4 July 2007
Published online 28 September 2007 in Wiley InterScience (www.interscience.wiley.com). DOI: 10.1002/jbm.a.31638

Abstract: Proper cell attachment and distribution, and thus stronger association *in vivo* between a bone implant and native tissue will improve the success of the implant. In this study, the aim was to achieve promotion of attachment and uniform distribution of rat mesenchymal stem cell-derived osteoblasts by introducing chemical and topographical cues on poly(3-hydroxybutyrate-*co*-3-hydroxyvalerate) (PHBV) film surfaces. As the chemical cues, either alkaline phosphatase was covalently immobilized on the film surface to induce deposition of calcium phosphate minerals or fibrinogen was adsorbed to improve cell adhesion. Microgrooves and micropits were introduced on the film surface by negative replication of micropatterned Si wafers. Both chemical cues improved cell attachment and even distribution on the PHBV films, but Fb was more effective especially when combined with the micropatterns. Cell alignment ($<10^\circ$ deviation angle) parallel to chemically modified microgrooves (1, 3, or 8 μm groove width) and on 10 μm-thick Fb lines printed on the unpatterned films was achieved. The cells on unpatterned and 5 μm-deep micropitted films were distributed and oriented randomly. Results of this study proved that microtopographies on PHBV can improve osseointegration when combined with chemical cues, and that microgrooves and cell adhesive protein lines on PHBV can guide selective osteoblast adhesion and alignment. © 2007 Wiley Periodicals, Inc. J Biomed Mater Res 85A: 1001–1010, 2008

Key words: PHBV; photolithography; micropatterned films; osteoblasts; bone tissue engineering

INTRODUCTION

Bone tissue engineering is becoming more promising for the replacement or repair of damaged bone because advanced techniques such as micro and nanotechnology are now being used more extensively to form tissues that closely mimic the microstructure and function of the natural tissue.

Biodegradable polymers are considered to be the most suitable materials for scaffold preparation because of their variety, versatility, and biodegradability. When applied, these materials circumvent the need for device removal from the body.

Poly(3-hydroxybutyrate-*co*-3-hydroxyvalerate) (PHBV) is one of the naturally derived biodegradable polymers that has improved processing and mechanical properties with respect to PHB,[1,2] which is brittle and has a higher melting temperature.[3] Properties of PHBV such as glass transition temperature (T_g), stability, degradability, and crystallinity can be modified by changing its copolymer composition and molecular weight.[4–6] Therefore, the rate and extent of accumulation of degradation products, such as β-hydroxybutyric acid, which is a normal constituent of blood,[7–9] and hydroxyvaleric acid, at the site of implantation is not problematic for PHBV, unlike the faster degrading α-polyhydroxy acids of the polylactide family. PHBV can be processed to take on various shapes, forms, and porosities because its thermoplastic properties are suitable. Studies on using PHBV for bone tissue implants involved attempts to match the mechanical strength and form to that of bone through incorporation of minerals.[10,11] It can therefore be assumed that PHBV has a significant potential for use as a support for long-term bone regeneration *in vivo*. More recently, *in vitro* growth of osteoblasts on macroporous, three-dimensional PHBV matrices has been reported.[12] Suitability of the matrices for bone tissue engineering was shown by an increase in osteocalcin expression and alkaline

Correspondence to: V. Hasirci; e-mail: vhasirci@metu.edu.tr
Contract grant sponsor: Scientific and Technical Research Council of Turkey (TUBITAK) TBAG; contract grant number: 2288
Contract grant sponsor: METU Graduate School of Natural and Applied Sciences; contract grant number: BAP-2004-07-02-00-15

phosphatase (ALP) activity over a 60-day period.[13] In addition, a comprehensive characterization of MC3T3-E1 S14 osteoblast growth and differentiation on nonporous PHBV films was carried out, in which the ability of PHBV to support osteoblast cell function was shown.[14] It is well known that initial cell attachment and proliferation are dependent on the functional groups of an implant surface rather than its bulk. Like most of the biodegradable polymers, PHBV lacks functional groups for cell attachment and needs to be modified. Uniform cell attachment, distribution, and thus stronger association between the implant and native tissue *in vivo*, would improve the success of the implant. Introducing cell adhesive patterns on a polymer surface or creating surface microtopography suitable for cell confinement are two methods that are applied for this purpose. Integrin transmembrane receptors of cells bind specific ECM components and the cytoskeleton.[15] Integrin-mediated cell adhesion influences subsequent cell processes, including spreading, proliferation, and differentiation via signaling pathways.[16,17] Surface topography of a material is known to be important in the cell–material interactions, for cell orientation and migration.[18] Osteoblastic phenotype and degree of bone contact were shown to be responsive to topography; polished surfaces produce less material–bone contact, and bone formation is preferentially observed in grooves and crevices.[19] Cells appear to recognize surface features and respond accordingly, possibly through reshaping of the actin filaments in filopodia. This is called contact guidance. When filopodia are presented with a favorable cue, they become stabilized through the action of tubulin microtubules and alignment of actin.[19–21] There is evidence that the symmetry or regularity of microscopic surface topographies play an important role in cellular responses.[22] Lithography has enabled researchers to fabricate surfaces with well-defined chemical and/or topographical patterns at the micro or nanoscale. These patterned materials could be used as templates to transfer these designs on polymeric surfaces through the use of a variety of methods such as molding, embossing, or solution casting. This could be used to study cell–substrate interactions with chemically or topographically patterned polymers of different chemistries, and understand how geometrical features influence osteoblast biology.[23,24] There are strong evidences to claim that micropatterning of osteoblasts in microgrooves leads to their alignment, and improves their activity, another desired property if the patterned film is used as a bone implant. Qu et al. reported that both micronscale pits and grooves stimulated matrix deposition and mineralization, possibly through different mechanisms.[24] Further evidence about the influence of surface topography on osseointegration has been provided using *in vitro* models,[25–27] and *in vivo* tests.[28] It was also reported for the first time that osteoblasts can be induced to align with the microgrooves on biodegradable PHBV-P(L/D,L)LA polymer films when fibrinogen (Fb) adsorbed on the surface was used as a chemical cue, and that this alignment could improve expression of the differentiated phenotype.[29]

The organs and tissues of the body are organized in specific three-dimensional architectures. Repair of such tissues, therefore, would be improved upon provision of 2D and 3D cues, because these would induce cells to assemble and organize in a style typical of the target organ or tissue. Thus, active biomaterials, carrying the cues required for induction of appropriate morphogenesis, may be designed. Various researchers have used a range of techniques to pattern substrates with specific surface chemistries to interact with the cells.[30–32] Microcontact printing was one of the earliest methods proposed. To our knowledge, there are no preceding studies reported in literature on osteoblast alignment to patterns of chemical cues generated on PHBV films.

This study aimed at promoting mesenchymal stem cell-derived osteoblast attachment to PHBV and their even distribution by introducing chemical and topographical cues on film surface. To serve as a chemical cue for osteoblasts, either Fb was adsorbed or ALP was covalently immobilized on the film surface and subsequently Ca-P minerals were deposited by enzymatic activity. Microgrooves and micropits were generated on the film surface as topographical cues. In addition to that, osteoblast alignment to a micropattern was evaluated; either films with microgrooves of different groove widths (1, 3, or 8 μm) were produced or Fb lines were microcontact printed on the unpatterned film surface. This study demonstrates that 3D and 2D patterns in the form of microgrooves and cell adhesive protein lines, respectively, on PHBV can guide osteoblast adhesion and alignment and further highlights the role of surface topography as a modulator of cell distribution.

MATERIALS AND METHODS

Production of micropatterned templates, PDMS stamp, and polymer films

Single crystal silicon wafers were used to create a variety of templates for studying the influence of pattern type on cell adhesion (Table I). The wafers were cut into 1.5 × 1.5 cm^2 pieces and cleaned with TCA (trichloroethane), ACE (acetone), and ISO (isopropyl alcohol). Thin films of SiN_x were grown on these slices by plasma-enhanced chemical vapor deposition. Subsequently, the slices were coated with positive photoresist for 40 s at a spin rate of 4000 rpm,

TABLE I
Properties of the Micropatterned Silicon Wafers

Wafer Parameters	Wafer Micropattern Dimensions (μm)				
	MG1	MG2	MG3	MCP	MP
Groove width	1	1	1	10	4
Ridge width	1	3	8	40	10 and 20
Groove depth	30	30	30	10	5
Inclination angle of the side walls (°)	54.7	54.7	54.7	90	90

MG: microgrooved template; MCP: template used to prepare the stamp for microcontact printing; MP: micropitted template.

and by using a photomask, exposed to UV light of 6 mW for 25 s in the Karl Suss Mask aligner. The photoresist film was developed for 40 s in a solution of 1:4 developer and deionized water. The pattern on the mask was transferred to the SiN_x layer by hydrofluoric acid (HF) etching of the exposed SiN_x for 60 s. The photoresist was removed off the wafer with acetone. For the production of microgrooved (MG) Si templates, the exposed parts of the wafers were etched to the desired depth in a KOH solution that was heated to 40°C and stirred at 600 rpm. Lastly, the remaining SiN_x layer was removed using dilute HF. The micropitted (MP) Si template and the template that was used for the preparation of the PDMS stamp were produced by reactive ion etching (RIE) instead of the KOH etching.

PDMS stamp was prepared by pouring the PDMS prepolymer–catalyst mixture on the MG template and its subsequent polymerization at 70°C. Resulting MG PDMS polymer was removed mechanically from the silicon template.

PHBV (with 8 mol % 3-hydroxyvalerate) films were prepared by solvent casting of 6% (w/v) solution of PHBV in dichloromethane on the micropatterned silicon (Si) templates and glass petri plates. Air-dried films were peeled off the template and glass surface.

Chemical modification of film surface

Fb was adsorbed on the air-dried micropatterned and unpatterned films following sterilization in EtOH (70%) for 2 h and PBS (pH 7.2, 10 m*M*) wash. Fb solution (1 mg/mL in PBS) was applied on the dry films. After 10 min, excess Fb solution was removed from the film surface by a pipette, and the films were left at room temperature to dry.

Microcontact printing of Fb to unpatterned PHBV surface was done to generate a 2D micropattern of adhesive protein lines. Surface of the PDMS stamp was exposed to 100 W O_2 RF plasma for 60 s to make its surface hydrophilic and then left in 70% ethanol for sterilization. After drying in the laminar hood, the stamp was immersed in Fb solution (1 mg/mL in PBS) for 30 min at room temperature. Finally it was dried in the laminar hood and placed in contact with the unpatterned, ethanol sterilized and slightly moist PHBV film, and incubated in the CO_2 incubator at 37°C for 15 min under a 50 g weight.

As the alternate chemical modification, ALP was covalently immobilized on micropatterned and unpatterned PHBV films to induce Ca-P deposition on the film surface. To activate the polymer for enzyme immobilization, the films were exposed to UV (λ = 313 nm, 75 W) for 2 h and then epichlorohydrin solution (4.3 mL 2*M* NaOH, 1 mL distilled H_2O, 0.1 mL epichlorohydrin) was applied on the film surface. Excess of the epichlorohydrin solution was withdrawn immediately with a pipette. The films were incubated for 15 min at 37°C and then washed in PBS (0.1*M*, pH 7) for 1 h in a shaking water bath at 37°C. These epichlorohydrin-modified films were sterilized in 70% EtOH for 2 h, washed with 50% EtOH for 30 min, and left in 2 mg/mL ALP solution (ALP in borate buffer, 0.2*M*, pH 9) overnight (17 h). Finally, the films were washed in PBS for 4 h and left to dry in a laminar flow cabinet. ALP immobilization was confirmed by indirect immunostaining using monoclonal anti-ALP antibody and FITC-labeled secondary antibody. To induce Ca-P deposition on the film surface by the enzyme ALP, the films were incubated in 1 mL Tris buffer (pH 7.4, 25 m*M*) solution containing 24 m*M* Ca^{+2}, 0.5 m*M* Mg^{+2}, 142 m*M* NaCl, and 12.5 m*M* β-glycerophosphate, at 37°C for 90 h. The Tris buffer was refreshed on the second day of incubation. Ca-P deposition was examined using SEM.

In vitro studies

Isolation of bone marrow mesenchymal stem cells

Young adult Sprague–Dawley rats were euthanized by diethyl ether inhalation, their femurs and tibia were excised, and the bone marrow was flushed out with primary medium (DMEM containing 20% FBS and 100 U/mL penicillin and 100 μg/mL streptomycin) using a syringe, centrifuged (5 min, 500 g), resuspended in primary medium, and plated in T-75 flasks (cells from one femur per flask).[12] These primary cultures were incubated in a carbon dioxide incubator (Sanyo MCO-17 AIC, Japan) at 37°C and 5% CO_2, washed with PBS after 2 days, and their medium was changed every other day. First passage cells were cryopreserved in FBS containing 15% DMSO, thawed, and grown upon use.

Osteoblast culture on the films

Second passage mesenchymal stem cells grown in primary medium were seeded on unpatterned and micropatterned dry PHBV films (1.5×10^4 cells/cm^2), and grown for 24 h in a CO_2 incubator. At the end of 3 h following cell seeding, complete medium (primary medium supple-

mented with 10 m*M* β-glycerophosphate, 50 mg/mL L-ascorbic acid, and 0.9 μ*M* dexamethasone) was added on the films to promote osteoblastic differentiation of the marrow mesenchymal stem cells. Tissue culture polystyrene (TCPS) served as the positive control. MTS assay, which measures cell metabolism, was carried out 24 h after cell seeding to approximate the number of cells attached on the film surface. The films were transferred into clean wells and the cell number on each sample was determined in triplicate. MTS/PMS reagent (0.5 mL low glucose DMEM containing 10% MTS/PMS) was added on the films and then incubated for 2 h at 37°C in the CO_2 incubator.[13] Absorbance of the medium from each sample was determined at 490 nm using Elisa Plate Reader (Maxline, Molecular Devices, USA). Cell number was determined using an MTS calibration curve generated by the same protocol.

Osteoblast alignment to the micropattern

Bone marrow mesenchymal stem cells were seeded on PHBV films at low density (at a concentration of 2.5×10^4 cells/mL, 1000 cells/film) where cell-to-cell contact was minimized, and grown for 4 days in complete medium. The cells were fixed with 2.5% glutaraldehyde (in 0.1*M*, pH 7.4, sodium cacodylate buffer) for 2 h and stained with acridine orange for 10 min. Using the images recorded at 480 nm excitation, a line was drawn along the long axis of a cell and the angle with respect to the axis of the micropattern was measured (0° indicates perfect alignment, 90° indicates orthogonal to the channel axis). On the unpatterned films and the films with micropits, an arbitrary line was drawn to serve as the reference axis. Angles of deviation from the groove axis (on MG films) or the arbitrary line (on unpatterned and MP films) were determined.

RESULTS AND DISCUSSION

PHBV films with a micropatterned surface were prepared to study the influence of topography and the chemical cues on cell attachment, organization, and alignment. Three MG Si templates with different ridge widths and one MP Si template with alternating pattern of two pits of different sizes (Table I) were produced by photolithography and subsequent surface etching. MG templates were produced by wet etching, which results in sloping walls. On the MP template, the isotropic wet etching with KOH did not allow achievement of the desired depth, and therefore, RIE, which leads to vertical walls, was used instead.

Solvent casting of PHBV on micropatterned master templates resulted in an inverted pattern generation on the film surface. The whole approach used to obtain chemical and physical cues on the polymer surface is summarized in Figure 1.

Efficiency of Fb adsorption on MG films was evaluated using FITC-labeled Fb. Resulting fluorescence

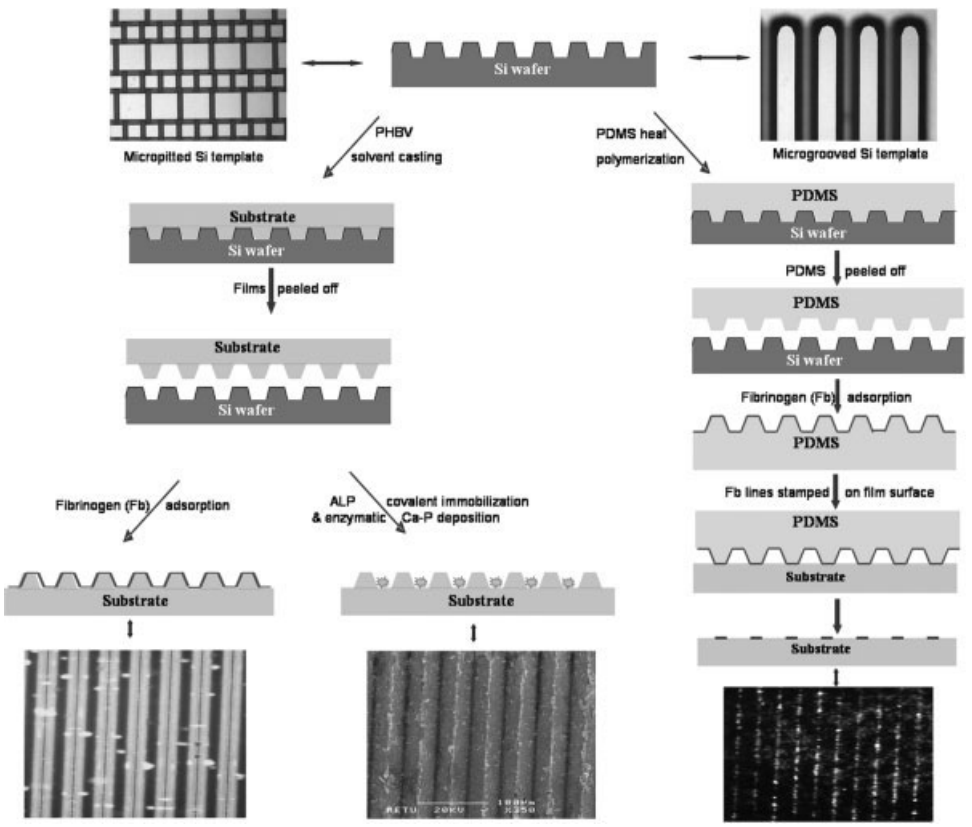

Figure 1. Schematic presentation of the methods used for film surface modification.

microscopy images verified that Fb adsorbed more intensely on the side walls of the grooves (Fig. 1).

Microcontact printing of FITC-Fb on unpatterned PHBV surface resulted in protein lines that were discontinuous at some points (Fig. 1). This incomplete transfer of Fb may be attributed to the hydrophobic nature of PHBV, which does not promote protein adsorption in a dry state.

In native bone tissue, the extracellular matrix (ECM) consists mainly of collagen type I and hydroxyapatite crystals embedded among these collagen fibers. It is known that the ALP enzyme present in the ECM of bone is involved in the formation of hydroxyapatite crystals by providing free phosphate groups to the environment. To imitate this natural process, we immobilized the ALP to PHBV film surface and induced deposition of Ca-P by this enzyme to generate a natural microenvironment for the osteoblasts. ALP was successfully immobilized on the PHBV films (Fig. 2). It was confined within the grooves of MG films [Fig. 2(d)] while its distribution on MP films could not be discerned clearly [Fig. 2(c)], and on unpatterned films it was randomly distributed. It is the epichlorohydrin spacer that links the ALP enzyme to the polymer film surface, and it was hypothesized that by localizing epichlorohydrin solution only within the grooves and pits it would be feasible to confine the enzyme at these particular locations. This, in turn, would lead to patterned enzymatic deposition of Ca-P, which is expected to promote selective osteoblast attachment. The method used to localize the epichlorohydrin spacer within the grooves and pits was removal of excess fluid from the film surface by a pipette and concentrating the epichlorohydrin in the grooves and pits by surface tension. Although it worked for the deeper, MG films, this was not effective for the shallower, MP PHBV. This result suggests that the important parameters to take into consideration in this method for a successful localization are the depth and type of the patterns. It was not possible to localize the epichlorohydrin within the pits because they were too shallow (six times more shallow compared with the microgrooves) or simply it was the effect of the pattern; removal of excess fluid from the film surface by a pipette may not be an effective method for MP films.

Ca-P deposition on ALP-immobilized films was initiated by phosphate removal from an organic material, β-glycerophosphate, by the immobilized enzyme. Substantial Ca-P deposition was observed in some parts of the film surface [Fig. 2(e,f)] while it was difficult to detect its presence in others. Although ALP was localized within the grooves of MG films, mineralization was observed both in

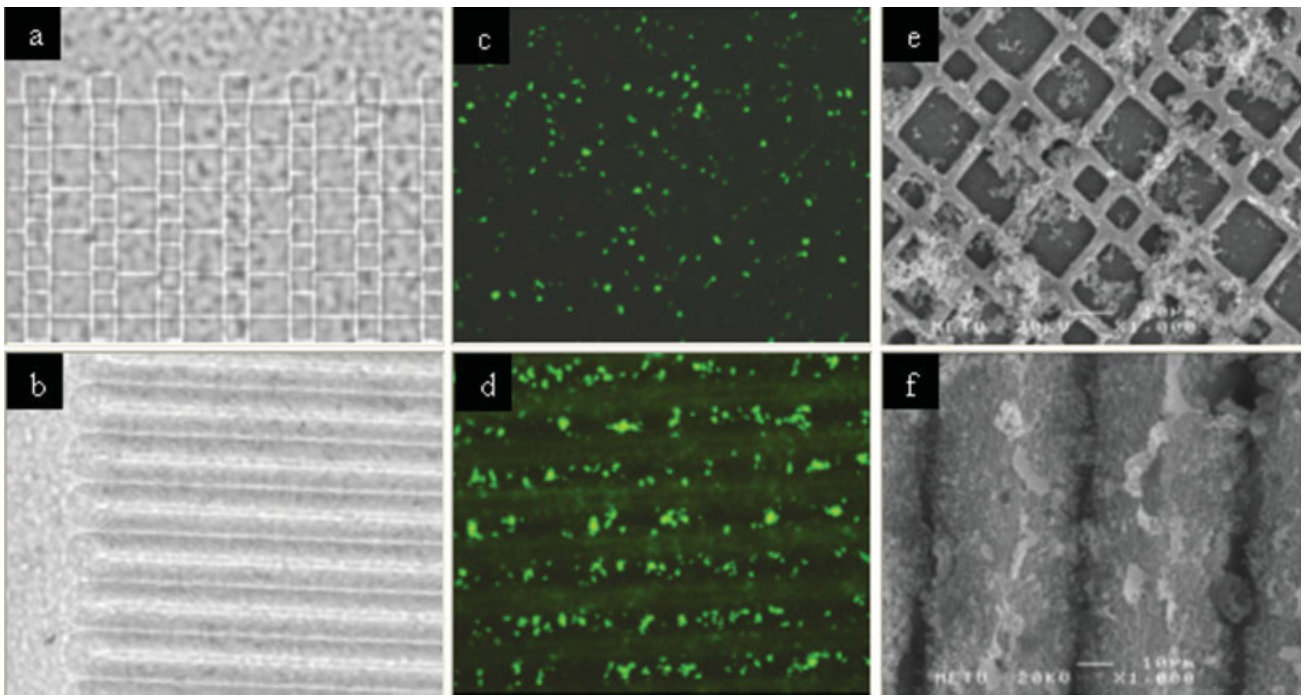

Figure 2. Images taken at particular steps of the sequential method used for enzymatic Ca-P deposition on micropatterned PHBV films. (a) Untreated MP film (light micrograph, ×150), (b) untreated MG film (light micrograph, ×75), (c) alkaline phosphatase covalently immobilized on MP film (indirect immunostaining with FITC-labeled secondary antibody, ×150), (d) alkaline phosphatase covalently immobilized on MG film (indirect immunostaining with FITC labeled secondary antibody, ×150), (e) enzymatically deposited Ca-P minerals on MP film surface (SEM image, ×1000), and (f) enzymatically deposited Ca-P minerals on MG film surface (SEM image, ×1000). [Color figure can be viewed in the online issue, which is available at www.interscience.wiley.com.]

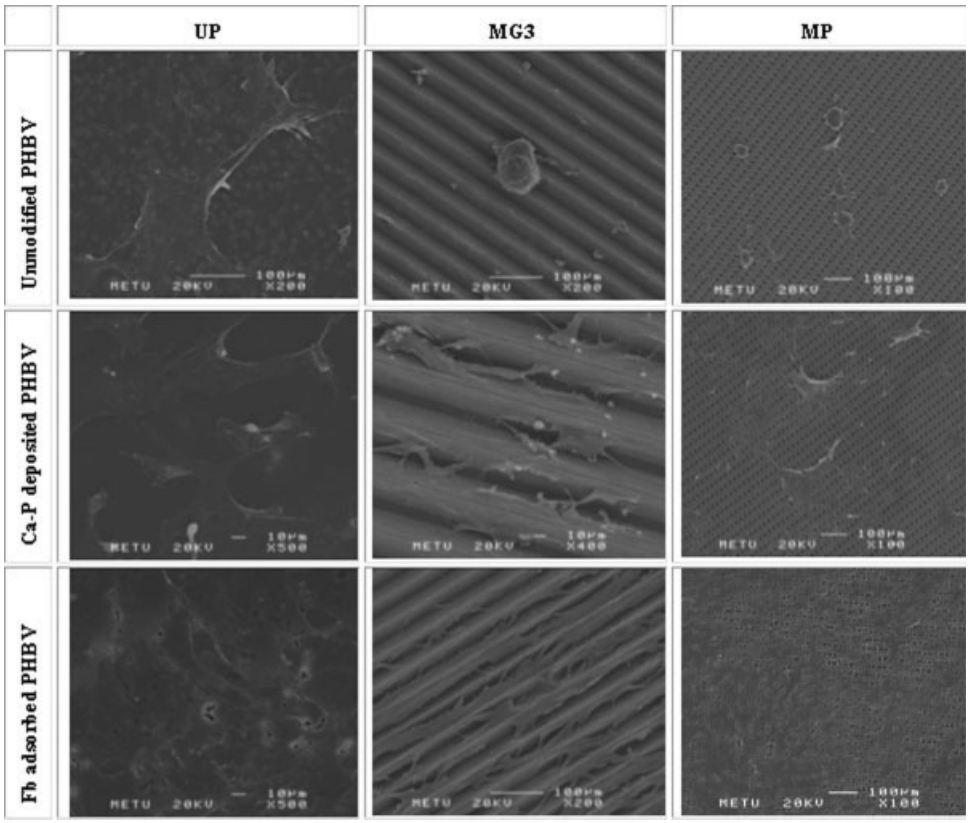

Figure 3. SEM images of osteoblast-seeded PHBV films, taken 4 days postseeding.

grooves and on the ridges. ALP activity was not the same on all films; a higher enzyme activity led to a turbid fluid formation due to excess Ca-P generation within that well. It has been reported by Ito et al. that hydroxyapatite can be readily deposited from a solution onto PHBV surfaces.[33] These outcomes indicate that even though ALP was immobilized within the grooves of MG films, the nonselective Ca-P deposition on the film surface may have been inevitable in the wells with excess Ca-P. MP films also had Ca-P formed both in the pits and on the ridges [Fig. 2(e)]. There is a need to develop a better method for immobilization of the ALP enzyme, such that the enzyme activity will not be affected, and by this way it will be more feasible to have a control over Ca-P generated and deposited.

Osteoblast morphology and distribution on PHBV films was evaluated using scanning electron microscopy (Fig. 3). In general, independent of the surface pattern, chemically unmodified films did not support cell attachment. Cells on the unpatterned, unmodified films formed clumps. Very few of the cells on the unmodified, MG films aligned parallel to the groove axis while most formed clumps. On the unmodified, MP films some spread cells were observed, but the majority formed clumps, too.

Chemical modification of film surface greatly improved cell attachment and uniformity of cell distribution. Improvement in the cell attachment is also revealed by MTS assay carried out 24 h after cell seeding (Fig. 4). Although presence of both Fb and Ca-P on the surface had positive effects, Fb with its RGD sequences for integrin attachment seems to be more effective, especially in the presence of micropatterns. Fb adsorption on MG films led to

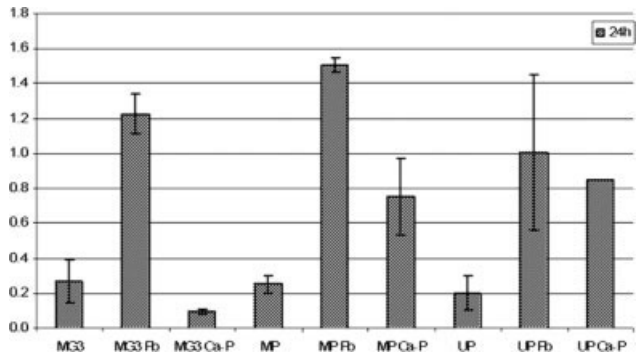

Figure 4. Cell attachment on PHBV films normalized to cell number on TCPS after 24 h, following cell seeding. MG3: Microgrooved 3; MG3 Fb: Fb adsorbed microgrooved 3; MG3 Ca-P: Microgrooved 3 with Ca-P deposition; MP: Micropitted; MP Fb: Fb adsorbed micropitted; MP Ca-P: Micropitted with Ca-P deposition; UP: Unpatterned; UP Fb: Fb adsorbed unpatterned; UP Ca-P: Unpatterned with Ca-P deposition.

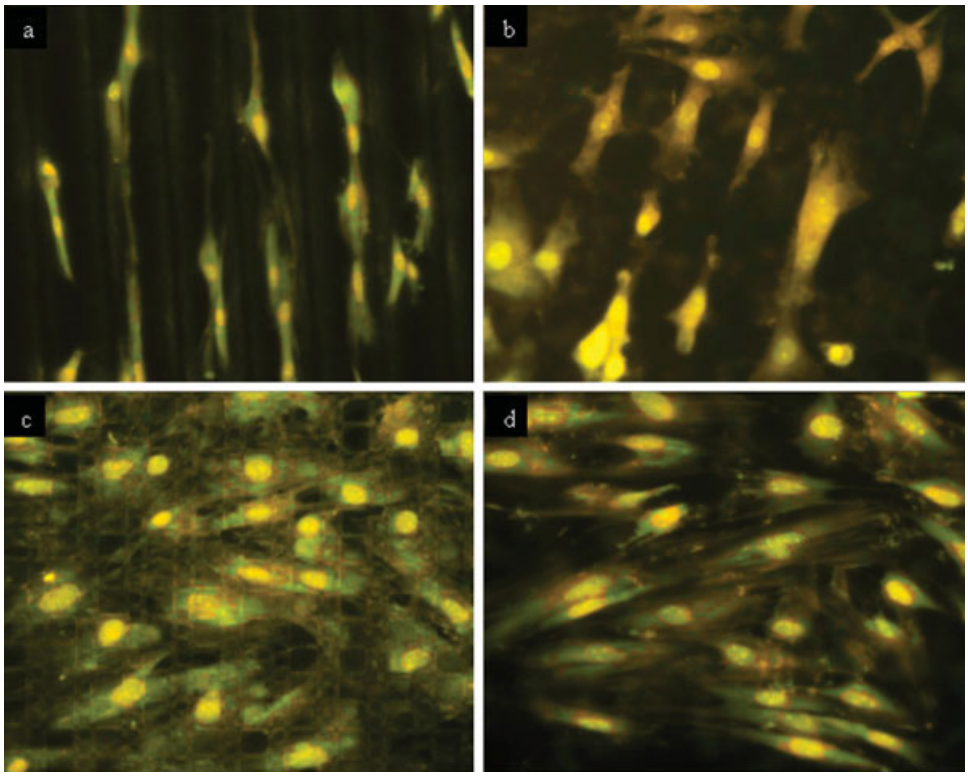

Figure 5. Osteoblast morphology on PHBV films with different surface treatment revealed by acridine orange staining. (a) Fb-adsorbed MG film (4 days postseeding, ×150), (b) Fb MCP film (4 h postseeding, ×300), (c) Fb-adsorbed MP film (4 days postseeding, ×150), (d) Fb-adsorbed UP film (4 days postseeding, ×150). [Color figure can be viewed in the online issue, which is available at www.interscience.wiley.com.]

osteoblast alignment along the groove axis. To some extent Ca-P deposition did the same, too. Osteoblasts on the MP films were not confined within the pits, either due to their size being too large relative to the pattern dimensions or due to the presence of Fb or Ca-P over the whole surface. However, regardless of the cell location, the presence of the patterns (micropits and microgrooves) on the film surface increased the number of cells attached on Fb-adsorbed films compared with their unpatterned counterparts (Fig. 4). Among the whole range of films prepared, Ca-P MG films showed the lowest cell attachment; however, 2-week MTS data (not shown) indicated that these films supported a cell number as high as the rest.

Cell alignment on the MG films and the cell spreading on MP and UP films were evaluated by fluorescence microscopy; fluorescence images of cells stained with acridine orange were obtained 4 days postseeding [Fig. 5(a,c,d)]. Osteoblasts aligned parallel to groove axis on all MG films; they required 1–3 days to do so. A number of previous studies, including our own, have focused on the contribution of microscale topographical cues to osteoblast alignment,[29,34–45] and fewer studies explored the same with regard to nanoscale topography.[46,47] The results obtained in this study are in accordance with the other reports on osteoblasts on micropatterned surfaces, such as with the finding by Perizzolo et al. of alignment of rat calvarial osteoblasts with the grooves after 24 h on Ti and HA coated Si MG templates with dimensions similar to the ones used in this study.[39]

Microcontact printing led to 2D chemical patterns on the unpatterned films. Only 4 h was enough to

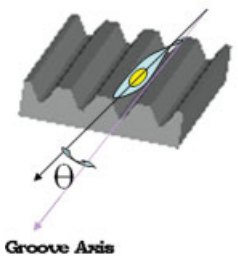

(a)

Chemical modification / Sample	Unmodified (θ)	Fb Adsorbed (θ)
MG1	0	3.32 ± 6.75
MG2	0	4.21 ± 7.73
MG3	0	4.66 ± 7.59
MP	–	37.08 ± 23.12
UP	41.82 ± 21.75	44.90 ± 25.36
TCPS	37.71 ± 30.35	

(b)

Figure 6. Method of (a) alignment determination and (b) the values of deviation angle of cells from groove axis on MG PHBV films and an arbitrary reference line on UP and MP PHBV films. [Color figure can be viewed in the online issue, which is available at www.interscience.wiley.com.]

observe cell alignment to Fb lines on these films. They were effective in aligning the osteoblasts, but the separation between the Fb strips, 40 μm, was not wide enough to prevent cells from crossing the neighboring lines or positioning themselves perpendicular to line axis, and this resulted in a decrease in the cell alignment [Fig. 5(b)]. It is possible to deduce from the image that when spread, the rat bone marrow derived MSC can be as long as about 80–90 μm, and this length should be considered as the minimum width of the space between the lines in order to get cells attached and aligned only on the adhesive protein strips.

It was observed that nuclei of most of the cells on Fb-adsorbed MP films were localized within the large pits, but still the cell extensions were random and spanning over two or three micropits [Fig. 5(d)]. In a similar study, MG63 osteoblast-like cells cultured on titanium surfaces with hemispherical cavities with a diameter of 30 μm (ratio of cavity area vs. outside area was 6) were observed to anchor in adjacent cavities, one cell spanning a border between two adjacent cavities.[48] In another study, MG63 and SAOS-2 osteoblast-like cells grown on bioactive composite surfaces with a microwell width of 50 μm and a ridge width of 10 μm aligned along ridges and bridged across wells.[37] Thus, osteoblast cells tend to span over the borders of micropits of less than 50 μm width. In contrast, use of gap-cornered microwells seems to lead to osteoblast patterning. Rat calvarial osteoblasts seeded on epoxy resins with gap-cornered boxes (wells) of 34 μm width and 10 μm depth were shown to align along the walls of the boxes at 1 and 2 h, but by 4 h additionally began aligning diagonally within the boxes, and at 1 week the cell sheets were aligned diagonally with respect to the boxes.[38]

Cell alignment was determined quantitatively by measuring the angle of deviation from the groove axis (orientation angle) on MG films and the angle of deviation from an arbitrary reference line drawn on MP and UP film images (Fig. 6).

Although the difference was not significant, the deviation angle was observed to increase as the groove width, and thus the pitch of MG films, increased [Fig. 6(b)]. It was determined from the images of acridine orange stained cells on MG films that the cells attach to the inclined sidewalls of the grooves and only few of them could span the space between the two walls of a groove. Therefore, it was concluded that rather than the groove width (defined as the groove base width here) alone, the whole region between the two ridges is influential on the deviation angles observed with different MG films. Khakbaznejad et al. determined the orientation angle of rat calvarial osteoblasts on titanium-coated MG Si substrates with 30 μm groove depth, 47 μm pitch width, and inclined walls.[43] A nonconfluent monolayer of osteoblast-like cells up to and including the fourth day of incubation were observed and the mean orientation angle of these cells was $10.7^\circ \pm 0.8^\circ$ on the fourth day. The difference between the results of orientation angle on the MG films and the ones in that study can be explained as being due to the difference in cell density on the substrates (1×10^3 cells/cm^2 in the current study vs. 2×10^5 cells/cm^2), since the higher the density the higher is the cell number not in direct contact with the surface pattern. The difference in the cell carrier materials should be considered, too.

There were too few cells (1–6 in number) on the chemically unmodified MG films (seeding density 1×10^3 cells/film) and they were all spread parallel to groove axis. However, it was not possible to determine the deviation angle of the cells on the chemically unmodified MP films, because they all had a circular morphology. In general, the cells on unpatterned surfaces, including TCPS and MP films, spread randomly, which is indicated by the average 45° deviation angle obtained [Fig. 6(b)]. This random osteoblast spreading on unpatterned (smooth) surfaces was shown quantitatively in one of our previous publications,[29] and also by another group.[36]

CONCLUSION

Polymeric surfaces like PHBV need to be modified with functional groups that are recognized by the cells, in order to support cell attachment. Results of this study proved that microtopographies on PHBV can improve osseointegration when combined with chemical cues. Microgrooves and cell adhesive protein lines on PHBV were able to guide selective osteoblast adhesion and alignment. However, microgrooves were more effective in restricting cell attachment due to the presence of a physical constraint, opposed to Fb lines on unpatterned film surfaces. Use of such microgrooves in combination with bone implants may restore the anisotropic mechanical properties of a damaged bone through generation of an oriented ECM.

References

1. Chun YS, Kim WN. Thermal properties of blends of poly(hydroxybutyrate-*co*-hydroxyvalerate) and poly(styrene-*co*-acrylonitrile). J Appl Polym Sci 2000;77:673–679.
2. Liu WJ, Yang HL, Wang Z, Dong LS, Liu JJ. Effect of nucleating agents on the crystallization of poly (3-hydroxybutyrate-*co*-3-hydroxyvalerate). J Appl Polym Sci 2002;86:2145–2152.
3. Anderson AJ, Dawes EA. Occurrence, metabolism, metabolic role, and industrial uses of bacterial polyhydroxyalkanoates. Microbiol Rev 1990;54:450–472.

4. Gogolewski S. Resorbable polymers for internal fixation. Clin Mater 1992;10:13–20.
5. Gogolewski S, Jovanovic M, Perren SM, Dillon JG, Hughes MK. Tissue response and *in vivo* degradation of selected polyhydroxyacids: Polylactides (PLA), poly(3 hydroxybutyrate) (PHB), and poly(3-hydroxybutyrate-*co*-3-hydroxyvalerate) (PHB/VA). J Biomed Mater Res 1993;27:1135–1148.
6. Taylor MS, Daniels AU, Andriano KP, Heller J. Six bioabsorbable polymers: *In vitro* acute toxicity of accumulated degradation products. J Appl Biomater 1994;5:151–157.
7. An YH, Woolf SK, Friedman RJ. Pre-clinical in vivo evaluation of orthopaedic bioabsorbable devices. Biomaterials 2000; 21:2635–2652.
8. Hankermeyer CR, Tjeerdema RS. Polyhydroxybutyrate: Plastic made and degraded by microorganisms. Rev Environ Contam Toxicol 1999;159:1–24.
9. Holland SJ, Jolly AM, Yasin M, Tighe BJ. Polymers for biodegradable medical devices. II. Hydroxybutyrate–hydroxyvalerate copolymers: Hydrolytic degradation studies. Biomaterials 1987;8:289–295.
10. Galego N, Rozsa C, Sanchez R, Fung J, Vazquez A, Tomas JS. Characterization and application of poly(*b*-hydroxyalkanoates) family as composite biomaterials. Polym Test 2000;19:485–492.
11. Coskun S, Korkusuz F, Hasirci V. Hydroxyapatite reinforced poly(3-hydroxybutyrate) and poly(3-hydroxybutyrate-*co*-3-hydroxyvalerate) based degradable composite bone plate. J Biomater Sci Polym Ed 2005;16:1485–1502.
12. Kose GT, Kenar H, Hasirci N, Hasirci V. Macroporous poly (3-hydroxybutyrate-*co*-3-hydroxyvalerate) matrices for bone tissue engineering. Biomaterials 2003;24:1949–1958.
13. Kose GT, Korkusuz F, Korkusuz P, Purali N, Ozkul A, Hasirci V. Bone generation on PHBV matrices: An in vitro study. Biomaterials 2003;24:4999–5007.
14. Kumarasuriyar A, Jackson RA, Grondahl L, Trau M, Nurcombe V, Cool SM. Poly(β-hydroxybutyrate-*co*-β-hydroxyvalerate) supports *in vitro* osteogenesis. Tissue Eng 2005;11:1281–1295.
15. Degasne I, Basle MF, Demais V, Hure G, Lesourd M, Grolleau C, Mercia L, Chappard D. Effects of roughness, fibronectin, and vitronectin on attachment, spreading, and proliferation of human-osteoblast like cells (Saos-2) on titanium implants. Calcif Tissue Int 1999;64:499–507.
16. Sinha R, Morris F, Suken A, Shah S, Tuan R. Surface composition of orthopaedic implant metals regulates cell attachment, spreading, cytoskeletal organisation of primary human osteoblasts in vitro. Clin Orthop 1994;305:258–272.
17. Juliano RL, Haskill S. Signal transduction from the extracellular matrix. J Cell Biol 1993;120:577–585.
18. Burridge K, Chrzanowska-Wodnick M. Focal adhesions, contractility, and signaling. Annu Rev Cell Dev Biol 1996;12:463–518.
19. Gray C, Boyde A, Jones SJ. Topographically induced bone formation in vitro: Implications for bone implants and bone grafts. Bone 1996;18:115–123.
20. O'Connor TP, Bentley D. Accumulation of actin in subsets of pioneer growth cone filopodia in response to neural and epithelial guidance cues in situ. J Cell Biol 1993;123:935–948.
21. Curtis ASG, Wilkinson CDW. Topographical control of cells. Biomaterials 1997;18:1573–1583.
22. Curtis ASG, Casey B, Gallagher JO, Pasqui D, Wood MA, Wilkinson CDW. Substratum nanotopography and the adhesion of biological cells. Are symmetry or regularity of nanotopography important? Biophys Chem 2001;94:275–283.
23. Wilkinson CDW, Curtis ASG, Crossan J. Nanofabrication in cellular engineering. J Vac Sci Technol B 1998;16:3132–3136.
24. Qu J, Chehroudi B, Brunette DM. The use of micromachined surfaces to investigate the cell behavioural factors essential to osseointegration. Oral Dis 1996;2:102–115.
25. Wieland M, Textor M, Chehroudi B, Brunette DM. Synergistic interaction of topographic features in the production of bone-like nodules on Ti surfaces by rat osteoblasts. Biomaterials 2005;26:1119–1130.
26. Anselme K, Bigerell M. Topography effects of pure titanium substrates on human osteoblast long-term adhesion. Acta Biomater 2005;1:211–222.
27. Huang HH, Ho CT, Lee TH, Lee TL, Liao KK, Chen FL. Effect of surface roughness of ground titanium on initial cell adhesion. Biomol Eng 2004;21:93–97.
28. Hallgren C, Sawase T, Ortengren U, Wennerberg A. Histomorphometric and mechanical evaluation of the bone-tissue response to implants prepared with different orientation of surface topography. Clin Implant Dent Relat Res 2001;3:194–203.
29. Kenar H, Kose GT, Hasirci V. Tissue engineering of bone on micropatterned biodegradable polyester films. Biomaterials 2006;27:885–895.
30. Mrksich M, Chent CS, Xia Y, Diket LE, Ingbert DE, Whitesides GM. Controlling cell attachment on contoured surfaces with self-assembled monolayers of alkanethiolates on gold. Proc Natl Acad Sci USA 1996;93:10775–10778.
31. Matsuda T, Sugawara T. Development of surface photochemical modification method for micropatterning of cultured cells. J Biomed Mater Res 1995;29:749–756.
32. Folch A, Toner M. Microengineering of cellular interactions. Annu Rev Biomed Eng 2000;2:227–256.
33. Ito Y, Hasuda H, Kamitakahara M, Ohtsuki C, Tanihara M, Kang IK, Kwon OH. A composite of hydroxyapatite with electrospun biodegradable nanofibers as a tissue engineering material. J Biosci Bioeng 2005;100:43–49.
34. Matsuzaka K, Walboomers XF, Ruijter JE, Jansen JA. The effect of poly L-lactic acid with parallel surface micro groove on osteoblast-like cells in vitro. Biomaterials 1999;20:1293–1301.
35. Matsuzaka K, Walboomers XF, Yoshinari M, Inoue T, Jansen JA. The attachment and growth behavior of osteoblast-like cells on microtextured surfaces. Biomaterials 2003;24:2711–2719.
36. Matsuzaka K, Yoshinari M, Shimono M, Inoue T. Effects of multigrooved surfaces on osteoblast-like cells in vitro: Scanning electron microscopic observation and mRNA expression of osteopontin and osteocalcin. J Biomed Mater Res A 2004; 68:227–234.
37. Rea SM, Brooks RA, Schneider A, Best SM, Bonfield W. Osteoblast-like cell response to bioactive composites-surface-topography and composition effects. J Biomed Mater Res B Appl Biomater 2004;70:250–261.
38. Hamilton DW, Wong KS, Brunette DM. Microfabricated discontinuous-edge surface topographies influence osteoblast adhesion, migration, cytoskeletal organization, and proliferation and enhance matrix and mineral deposition in vitro. Calcif Tissue Int 2006;78:314–325.
39. Perizzolo D, Lacefield WR, Brunette DM. Interaction between topography and coating in the formation of bone nodules in culture for hydroxyapatite- and titanium-coated micromachined surfaces. J Biomed Mater Res 2001;56:494–503.
40. Chehroudi B, McDonnell D, Brunette DM. The effects of micromachined surfaces on formation of bonelike tissue on subcutaneous implants as assessed by radiography and computer image processing. J Biomed Mater Res 1997;34: 279–290.
41. Lu X, Leng Y. Quantitative analysis of osteoblast behavior on microgrooved hydroxyapatite and titanium substrata. J Biomed Mater Res A 2003;66:677–687.
42. Ber S, Torun Kose G, HasVrcV V. Bone tissue engineering on patterned collagen films: An in vitro study. Biomaterials 2005;26:1977–1986.

43. Khakbaznejad A, Chehroudi B, Brunette DM. Effects of titanium-coated micromachined grooved substrata on orienting layers of osteoblast-like cells and collagen fibers in culture. J Biomed Mater Res A 2004;70:206–218.
44. Tan J, Saltzman WM. Biomaterials with hierarchically defined micro- and nanoscale structure. Biomaterials 2004;25:3593–3601.
45. Wang JH, Grood ES, Florer J, Wenstrup R. Alignment and proliferation of MC3T3-E1 osteoblasts in microgrooved silicone substrata subjected to cyclic stretching. J Biomech 2000; 33:729–735.
46. Zhu B, Lu Q, Yin J, Hu J, Wang Z. Alignment of osteoblast-like cells and cell-produced collagen matrix induced by nanogrooves. Tissue Eng 2005;11:825–834.
47. Lenhert S, Meier M-B, Meyer U, Chi L, Wiesmann HP. Osteoblast alignment, elongation and migration on grooved polystyrene surfaces patterned by Langmuir-Blodgett lithography. Biomaterials 2005;26:563–570.
48. Zinger O, Zhao G, Schwartz Z, Simpson J, Wieland M, Landolt D, Boyan B. Differential regulation of osteoblasts by substrate microstructural features. Biomaterials 2005;26:1837–1847.